

A methodology for the development of a Hinged Ankle-Foot Orthosis compatible with natural joint kinematics

*Original*

A methodology for the development of a Hinged Ankle-Foot Orthosis compatible with natural joint kinematics / Ferraresi, C., De Benedictis, C., Maffiodo, D., Franco, W., Peluso, A., Leardini, A.. - ELETTRONICO. - 73:(2019), pp. 93-102. (IFTToMM WC 2019 Cracovia (Polonia) 30/06/2019 - 04/07/2019) [10.1007/978-3-030-20131-9\_10].

*Availability:*

This version is available at: 11583/2738792 since: 2023-10-02T13:47:17Z

*Publisher:*

Springer Netherlands

*Published*

DOI:10.1007/978-3-030-20131-9\_10

*Terms of use:*

This article is made available under terms and conditions as specified in the corresponding bibliographic description in the repository

*Publisher copyright*

Springer postprint/Author's Accepted Manuscript

This version of the article has been accepted for publication, after peer review (when applicable) and is subject to Springer Nature's AM terms of use, but is not the Version of Record and does not reflect post-acceptance improvements, or any corrections. The Version of Record is available online at: [http://dx.doi.org/10.1007/978-3-030-20131-9\\_10](http://dx.doi.org/10.1007/978-3-030-20131-9_10)

(Article begins on next page)

# A methodology for the development of a Hinged Ankle-Foot Orthosis compatible with natural joint kinematics

Carlo Ferraresi<sup>1</sup> [0000-0002-9703-9395], Carlo De Benedictis<sup>1</sup>[0000-0003-0687-0739], Daniela Maffiolo<sup>1\*</sup>[0000-0002-5831-8156], Walter Franco<sup>1</sup>[0000-0002-0783-6308], Andrea Peluso<sup>1</sup>, Alberto Lear-dini<sup>2</sup>[0000-0003-3547-7370]

<sup>1</sup> Department of Mechanical and Aerospace Engineering, Politecnico di Torino, Torino, Italy

<sup>2</sup> Movement Analysis Laboratory, Istituto Ortopedico Rizzoli, Bologna, Italy

daniela.maffiolo@polito.it

**Abstract.** This work presents a new concept to design Hinged Ankle-Foot Orthoses (HAFOs), based on the definition of a special mechanical articulation able to mimic the physiological behavior of the human ankle joint. Current commercial braces typically do not take into account the natural variability of the ankle joint axis. As the hinge location as well as the rotation axis variability are both relevant for the overall function of the device, and strongly depend on the subject-specific characteristics, a methodology for the development of a HAFO with a floating axis of rotation, based on the in-vivo kinematic analysis of the ankle joint, is here proposed. The kinematic analysis was performed by calculation of the instantaneous and mean helical axes over the collected stereo-photogrammetric data of joint motion. This procedure was tested on a healthy subject, leading to the design and fabrication of a first customized prototype of the orthosis. The performance of this HAFO was experimentally verified by motion analysis. All relevant results are presented, and further possible future improvements of the procedure are discussed.

**Keywords:** ankle-foot orthosis, ankle joint kinematics, customized orthosis, instantaneous helical axis, mean helical axis, in-vivo kinematics, additive manufacturing of orthosis.

## 1 Introduction

Ankle-Foot Orthoses (AFOs) are widely prescribed to treat several deficits of the lower limb, such as drop foot, club foot, nervous and musculoskeletal disorders. In Hinged Ankle-Foot Orthoses (HAFOs) a mechanical hinge allows the rigid rotation between an upper shell tied to the shank and a lower part tied to the foot. The relative motion normally occurs only in dorsi-plantar flexion about a fixed axis defined by the position of the hinge, somehow orthogonal to the sagittal plane of the leg. The location of this hinge, because chosen not according to the specific anatomical and kinematic characteristics of the patient ankle, likely leads to unnatural patterns of motion at the ankle and at the other foot joints [1] and results in insufficient overall performance of the brace.

The complexity of the human ankle joint motion has been already outlined in several studies by means of different techniques [2-5], especially in-vitro or using invasive methodologies. In the present work, stereo-photogrammetric analysis was used in-vivo non-invasively to gather data about actual subject-specific ankle motion. This approach has been chosen due to its proved effectiveness and wide acceptance, though the results will be affected by well-known critical artifacts such as the instrumental errors and the motion of the soft tissues with respect to the underlying bone [6]. The kinematic analysis of human joints, as well as the evaluation of the performance of a HAFO during dynamic tasks (i.e. walking), can be performed by means of the calculation of the instantaneous (IHAs) and mean helical (MHAs) axes, which provide a robust quantitative assessment of the floating axis of joint rotation. The same methodology, previously used also for in-vitro analyses [7], can be hence adopted under specific assumptions to perform a preliminary evaluation of the natural joint kinematics, for the subsequent subject-specific design and for the functional evaluation of the HAFO.

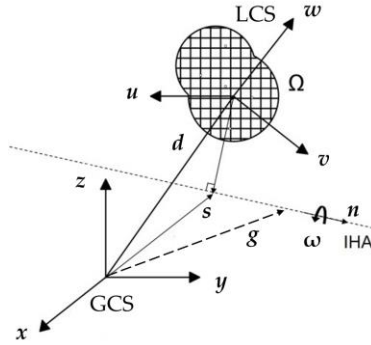
Considering that position and orientation of the IHA varies over time, from position to position, and in order to overcome the limits of the commercial braces available, a novel methodology for the design of a HAFO respectful of the natural joint kinematics has been proposed. This procedure includes the preliminary in-vivo kinematic analysis of the subject's ankle joint, which is performed by calculation of IHAs and MHAs since stereo-photogrammetric data, and the subsequent design and development of a brace prototype with a novel 6 Degrees of Freedom (DOFs) mechanical articulation, customized considering the anatomical and functional characteristics of the patient. The methodology has been outlined and exploited on a single healthy volunteer, and in this paper is presented and discussed. The architecture of the novel mechanical hinge, allowing more natural patterns of motion at the ankle thus providing functional protection to the joint, is described, and a first prototype of the brace is presented. Finally, the effectiveness of the orthosis was evaluated in-vivo by performing an additional kinematic analysis on the same subject, this time also wearing the subject-specific HAFO. The outcomes of the analyses are discussed, then future developments of this research are presented.

## **2 The in-vivo kinematic analysis of the ankle joint**

### **2.1 Methodology for the instantaneous and mean helical axis calculation**

The methodology for the kinematic analysis adopted in this work is based on the instantaneous (IHA) and mean (MHA) helical axes calculation, already proposed time ago for biomechanical research [5, 8, 9] and applied in a large number of ankle studies [7, 10]. The relative movement between two rigid bodies is described by a translation along and a rotation about the helical axis, whose position and orientation can change in time. These set of IHAs, called 'axode', can be processed in order to calculate the MHA, representative of the entire motion task. The accurate analytical description of these procedures for IHA and MHA calculation at the ankle in-vivo had been reported by these authors [10].

Figure 1 shows the parameters needed to represent the IHA and the motion of the local coordinate system (LCS), embedded with the body  $\Omega$ , with respect to the global coordinate system (GCS).  $\omega$  is the angular velocity vector, while the  $s$  and  $n$  vectors are required to define the position and orientation of the axis. Such parameters are given by solving the relations reported in Eq. (1-3):



$$\omega \times \dot{d} = (|\omega|^2 I - \omega \cdot \omega^T)(g - d) \quad (1)$$

$$s = d + \frac{1}{|\omega|^2}(\omega \times \dot{d}) \quad (2)$$

$$n = \frac{\omega}{|\omega|} \quad (3)$$

Fig. 1. IHA parameters.

in which  $g$  and  $d$  are respectively the position of an arbitrary point belonging to the helical axis and the location of the LCS origin, both expressed in the GCS. The dot notation represents the time derivative (approximated by the symmetric difference formula in the numerical procedure). The calculation of each parameter is performed for every time frame considered, thus providing a set of axes needed for the analysis.

The kinematic data are collected directly by means of a stereo-photogrammetric system (e.g. Vicon Motion Capture, Oxford), with eight digital cameras sampling at 100 Hz. The marker position protocol used is detailed in [11], but only the following few markers were relevant for the present kinematic reconstruction: HF-head of the fibula, LM-lateral malleolus, MM-medial malleolus, CA-calcaneus, FM-first metatarsal head, SM-second metatarsal head, and VM-fifth metatarsal head (Fig. 2). The additional markers presented in [11] are necessary for the static calibration as well as for the calculation of other joint rotations.

At first, the processing procedure performs the calculation of each marker 3D positions in a LCS, i.e. the shank reference frame. This frame has: the origin located at the intermalleolar segment mid-point; the  $v$  axis as the inter-malleolar (directed from lateral to medial); the  $u$  axis perpendicular to the quasi-frontal plane defined by the two malleoli and HF; the  $w$  axis orthogonal to the  $uv$  plane (Fig. 2). Then, an ideal rigid model of the foot is defined and calculated by means of a weighted least squares procedure: this is essential for IHA calculation as it is necessary to reduce the effects of the errors implied in the experiment, i.e. deformation of the foot marker cluster for instrumental and soft tissue artifacts. The minimization procedure performs iteratively until the maximum number of iterations (40) is reached or when the increase in the model parameters falls under a specific threshold. In our analyses, it was always kept under  $10^{-4}$  mm, thus resulting in an almost as negligible value. This methodology was originally conceived for rigid body motion and requires an optimization iterative processing of the measured marker coordinates. At the end of this iterative procedure, the 6 DOFs of the rigid foot

model are calculated in terms of the attitude vector (representative of 3D rotation about a single axis) and of the translation vector (i.e. the foot marker-set centroid with respect to the shank LCS), thus leading to the three rotational and three translational DOFs.

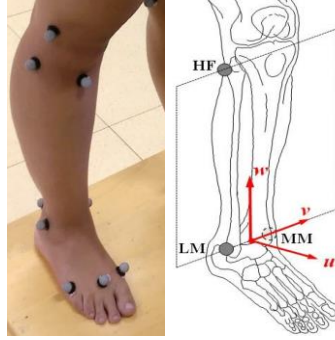


**Fig. 2.** Marker positioning for ankle joint kinematic (left) and the shank LCS (right).

After filtering, the time-histories of these DOFs are processed in order to calculate the parameters of the IHA. The IHA axode is then used to calculate the MHA over the whole time-frame by a least-square minimization process. This final calculation is crucial since the linear and angular dispersion parameters are thus calculated, providing a quantitative and concise assessment of the variability of the ankle joint motion.

## 2.2 Preliminary evaluation of the subject's ankle functionality

The methodology proposed in the previous section has been applied to evaluate the ankle kinematics of a healthy female volunteer, 28 years old.

Only a single subject has been considered, due to the preliminary characteristic of the study. In fact, aim of the work was to define and discuss a complete procedure that, starting from the in-vivo determination of the natural ankle kinematics, led to the realization of a customized brace. Once consolidated, it will be possible to apply such procedure to different subjects to verify its robustness.

Motion analysis data were collected during active plantar- and dorsi-flexion against gravity and level walking tasks, in barefoot condition. In the former task, the subject was asked to move in the sagittal plane the suspended foot from a high sitting position, without any constraint to motion. This task (I) was analyzed because it would be easily reproducible in any subject, also injured, because not requiring any locomotion ability. Of course, this task differs significantly from the typical condition in which the orthosis is used, that is in weight-bearing conditions. For this reason, walking trials were also analyzed (task II), in which the subject was asked to walk at natural speed in the laboratory. This task can be considered as more representative of the final application of the brace, but the effects of the gait dynamics on the joint kinematics, as well as on the more relevant effect of soft tissue artifact (as evidenced experimentally), should be taken into account during the analysis of this data.

For each motion task, several repetitions were collected and the data used to calculate the instantaneous and mean helical axes, as well as the linear  $d_{\text{eff}}$  and angular  $\chi_{\text{eff}}$

dispersion parameters (reported in Table 1). Figure 3 shows an example of the IHAs calculated for a level walking trial, in barefoot condition. The thick black line represents the MHA calculated for the specific task, carrying relevant information about the position and orientation of the MHA. The present experimental analysis confirmed that the axis of rotation of the ankle joint significantly differs from the conventional fixed one selected in many commercial braces [5]. The MHA did not coincide in fact with the inter-malleolar axis in any of the trials here analyzed, proving the need for a different concept of the mechanical articulation to be introduced in the HAFOs, able to adapt the relative motion between the foot and shank shells to the underlying limb segments. The values of linear and dispersion parameters calculated and presented in Table 1 were significantly higher than the those reported in the literature [7], but it should be taken into account that the approach presented in this work is affected by many uncertainties typical of any in-vivo motion analysis experiment, as the soft tissue artifact effect, which can be more easily kept under control during in-vitro analyses, i.e. because of bone pin attachments.

**Table 1.** Dispersion parameters of the IHAs axode calculated in barefoot condition.

Tasks	$d_{\text{eff}}$ [mm]	$\chi_{\text{eff}}$ [deg]
Active plantar- and dorsi- flexion	$21.9 \pm 1.1$	$32.9 \pm 0.3$
Level walking	$21.9 \pm 2.9$	$37.2 \pm 2.1$

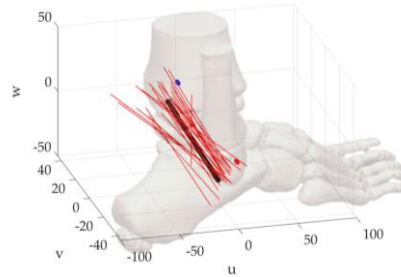


**Fig. 3.** Axode of IHAs (red line segments) in a walking trial. The malleoli (thick dots) and the MHA (thick black line) are shown. All axis units are in mm.

Whereas the critical aspects of the methodology will be discussed in Section 4, providing future improvements of the technique, the considerable variability of the rotation axis position during joint motion was confirmed consistently for each motion task performed, and therefore it should not be neglected within the design process of a HAFO. For this purpose, given the set of MHAs produced by the processing of the entire set of motion tasks, it is possible to find a general mean configuration of the ankle joint rotation axis, which can be used to define the basic features of the mechanical hinge.

### 3 The design and testing of the HAFO prototype

#### 3.1 A novel 6 DOFs hinge and the manufacturing of the HAFO prototype

A new mechanical articulation was designed with the aim of connecting the two shells of the HAFO in a way to allow an appropriately limited six degrees of freedom relative motion. The two main design goals of the articulation in between are i) the possibility to guarantee a physiological behavior of the ankle joint, and ii) the ability to compensate for any weaknesses in the natural containment structures. The first goal is reached by a floating axis of rotation connecting the two shells, so that their relative movement can follow the IHA of the natural ankle joint, regardless of the temporal evolution of the axode, and with a mean axis of the floating joint corresponding to natural ankle MHA. The second goal is obtained by favoring joint flexion-extension, while the out-of-sagittal-plane rotations are limited, namely prono-supination and abduction-adduction, as well as the three joint translations. The architecture of the mechanical articulation, under patent [12], will be briefly presented here below. A cross section sketch of the mechanical articulation is shown in Fig. 4; this was then manufactured by an assembly of corresponding stainless-steel components.

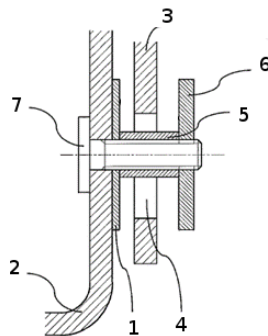


**Fig. 4.** A diagram of the cross section of the hinge; (1) inner plate, (2) foot shell, (3) outer plate + shank shell, (4) hole, (5) spacer, (6) threaded counter-plate, (7) connecting pin.

The components of the hinge are an inner plate 1 integral with the foot shell 2, an outer plate 3 integral with the shank shell (not visible in the figure) and provided with a hole 4, a spacer 5, a threaded counter-plate 6 and a connecting pin 7. This pin is integral with inner plate 1 and its head is in abutment on shell 2. The hole 4 of the outer plate has a diameter greater than the diameter of the spacer 5 to obtain a mutual radial clearance. Moreover, the distance between the inner plate 1 and the threaded counter-plate 6, determined by the length of the spacer 5, is greater than the thickness of the outer plate 3 to obtain a mutual axial clearance. This geometry allows the two shells to accomplish a relative movement with six degrees of freedom. The difference between the spacer 5 diameter and the outer plate hole 4 diameter allows three degrees of freedom in the sagittal plane to be accomplished. The difference between the thickness of the outer plate 3 and the distance between the inner plate 1 and the threaded counter-plate 6, set

by the length of the spacer 5, allows the further translation movements in the mediolateral direction and rotation movement in the frontal plane and in the transverse plane to be accomplished. The amplitudes allowed to the different natural movements, i.e. range of articular motion, except for the flexion-extension movement, can be determined and modified by simply defining the values of the length and outer diameter of the spacer 5 that is eventually fitted in each articulation. For comparison purposes, a 1 DOF configuration for the hinge is also obtained simply using an adequate spacer 5.

The orthosis shells have been fabricated by means of inexpensive and traditional techniques, i.e. directly modelling a layer of a thermoplastic material over the shank and foot of the subject. After cooling, metal plates (aluminum) have been riveted to the shank and foot shells in order to stiffen the device and to allow the assembly of the two HAFO components. The inner parts of the shells have been covered with padding to avoid direct contact with the skin and to distribute the contact pressure between the limb segments and the orthosis. A rubber sole has been glued to the lower external face of the foot shell to improve the comfort of the brace and the symmetry of the lower limbs, as the subject is normally wearing shoes. The complete prototype of the orthosis is shown in Fig. 5.



**Fig. 5.** Views of a prototype for the HAFO.

### 3.2 Experimental testing of the HAFO prototype

The shells have been provided with the holes required to mount the mechanical articulation, including both the intermalleolar and the MHA positioning solutions. Thanks to the possibility to fix the hinge in a 1 DOF configuration, three different set up were possible for the evaluation of the brace performance: B – inter-malleolar fixed axis of rotation; C – *anatomical* fixed axis of rotation, i.e. as given by the MHA; D – floating rotation axis, same mean positioning of the one in configuration C. The motion analysis trials performed to assess the behavior of the subject's ankle while wearing the HAFO were similar to the ones in barefoot condition (A), still considering the (I) active plantar- and dorsi-flexion and (II) level walking tasks, but they had to be carried out with a slightly different marker configuration: since the malleoli were hidden by the foot shell, the markers were placed 3 cm above and 1 cm behind the actual anatomical landmarks. The actual position of the malleoli was then reconstructed during post-processing. The

data produced by the motion capture system for each trial have been processed by means of the procedure reported in Section 2.1. The results, in terms of linear and angular dispersion data, are reported in Table 2.

**Table 2.** Dispersion parameters of the IHAs axode for all tasks (I – ankle plantar-dorsi flexion, II – walking) in different configurations (A – barefoot, B – fixed inter-malleolar axis of rotation, C – fixed anatomical axis of rotation, D – floating axis of rotation).

Trial	$d_{\text{eff}}$ [mm]	$\chi_{\text{eff}}$ [deg]	Trial	$d_{\text{eff}}$ [mm]	$\chi_{\text{eff}}$ [deg]
I – A	$21.9 \pm 1.1$	$32.9 \pm 0.3$	II – A	$21.9 \pm 2.9$	$37.2 \pm 2.1$
I – B	$28.9 \pm 1.3$	$17.6 \pm 0.1$	II – B	$40.1 \pm 4.9$	$28.2 \pm 1.6$
I – C	$27.6 \pm 0.4$	$23.3 \pm 2.9$	II – C	$60.8 \pm 10.6$	$34.4 \pm 5.2$
I – D	$31.6 \pm 2.4$	$17.4 \pm 1.1$	II – D	$48.5 \pm 4.2$	$36.4 \pm 1.7$

## 4 Discussion and future work

The IHAs reveal a considerable change in both position and orientation during each motion task, in each barefoot and HAFO configurations. However, the present analysis also shows dispersion parameters higher than those reported in the literature [7], though these were from in-vitro analyses. The significant increase of such parameters evidences a large variability of the IHA axode, thus providing inaccurate data for the kinematic evaluation of the ankle joint and for the resulting definition of the hinge position and orientation. To improve the accuracy of the methodology it would be necessary to reduce as much as possible the effect of undesired factors which negatively affect the axes calculation. In the in-vivo kinematic evaluation they would be represented mainly by the errors given by the soft tissue artifact and by the deformability of the foot marker cluster, resulting in an ill-posed definition of the rigid foot model. The methodology adopted, formerly conceived for rigid body motion analysis, requires specific optimization procedures in order to stiffen the marker-set on the foot. Due to the multi-segmental nature of the foot, as well as to the presence of instrumental errors and skin sliding, the resulting rigid foot model is likely not enough accurate to evaluate correctly ankle joint motion. It would be possible to overcome these critical points, thus leading to a more reliable methodology, by a better definition of the marker-sets: this can imply location of markers closer to the joint (avoiding placing markers on segments that change significantly their shape during motion, e.g. the forefoot), or directly on rigid shells fixed on body segments, so as to stiffen the cluster too.

Figure 6 shows an example of partial shells (i.e. without the integration of the mechanical articulation in the structure of the orthosis) connected to the shank and the foot, built with additive manufacturing, that will be adopted for further analyses. Among the several configurations of the mechanical articulation, the anatomical fixed (C) and floating (D) axis configurations did not emerge as the most effective, resulting in similar performance with respect to the fixed intermalleolar configuration (B). This unexpected result, that may be justified by the inaccurate design of the orthosis, given the uncertainty in the kinematic identification of the subject’s ankle joint, could be as-

cribed also to the unprecise manufacturing of the brace. The effectiveness of the orthosis is indeed affected by the shape of the shells, since the desired relative motion allowed by the hinge can be achieved only when good compatibility between the brace and the limb of the subject is guaranteed.



**Fig. 6.** Example of partial shells for the in-vivo analysis of ankle joint kinematics.

The brace shells manufacturing, that was performed by modelling of a thermoplastic material directly on the lower limb of a subject, led to a poor final result. This method was chosen for being not expensive and quick enough, but it did not allow to get an accurate reproduction of the subject's anatomy. This result points out the need for more advanced fabrication techniques. The manufacturing of the shells may be performed overcoming the traditional techniques and adopting for example 3D body scan methods to create a virtual positive cast of the limb, modelling the shells directly on the virtual scan, and fabricating the shells as well as the hinge by additive manufacturing with appropriate material [13,14]. Such procedure would provide a powerful tool for the customization of the brace, also taking into account potential foot deformity and specific needs of the patient. Additive manufacturing techniques would also allow to reconsider the whole fabrication process of the orthoses, for instance giving the possibility to the designer to create and implement the hinge directly during the 3D printing process, based on the specifications given by a previous kinematic analysis of the patient, as described here above.



**Fig. 7.** Views of a HAFO prototype 3D model obtained on the scan of the subject's limb.

In Fig. 7 a possible better solution for the architecture of the articulation and the shells, modeled directly on the 3D scan of the lower limb of the subject, is presented.

## 5 Conclusion

In this work a methodology for the development of a novel Hinged Ankle-Foot Orthosis has been proposed, focused on the quantitative analysis of the natural joint kinematics for each motion task performed by a single subject. The outcomes of this analysis (based on the calculation of IHA and MHA) have been used to define and implement a proposed novel 6 DOFs hinge into a custom-made HAFO prototype.

Although the study provided useful results for further analyses and for the development of the brace, some critical aspects were evidenced and require improvements. This concerns mainly the fabrication of the device and the optimization of the methodology for the in-vivo kinematic analysis. The adoption of 3D body scan and additive manufacturing techniques, as well as of a different positioning of the marker clusters on the body segments, shall lead to more accurate results and will be considered for future works.

## References

1. Leardini A., et al.: Multi-segment foot mobility in a hinged ankle-foot orthosis: the effect of rotation axis position. *Gait & Posture* 40(1), 274–277 (2014).
2. Van den Bogert A.J., Smith G.D., Nigg B.M.: In vivo determination of the anatomical axes of the ankle joint complex: an optimization approach. *J Biomech* 27(12), 1477–1488 (1994).
3. Giacomozzi C., et al.: Measurement device for ankle joint kinematic and dynamic characterisation. *Med Biol Eng Comput* 41(4), 486–493 (2003).
4. Imai K., et al.: In vivo three-dimensional analysis of hindfoot kinematics. *Foot Ankle Int* 30(11), 1094–1100 (2009).
5. Lundberg A., et al.: The axis of rotation of the ankle joint. *J Bone Joint Surg Br* 71(1), 94–99 (1989).
6. Leardini A., et al.: Human movement analysis using stereophotogrammetry. Part 3. Soft tissue artifact assessment and compensation. *Gait & Posture* 21(2), 212–225 (2005).
7. Leardini A., et al.: Kinematics of the human ankle complex in passive flexion; a single degree of freedom system. *J Biomech* 32(2), 111–118 (1999).
8. Stokdijk M., et al.: Determination of the optimal elbow axis for evaluation of placement of prostheses. *Clin Biomech* 14(3), 177–184 (1999).
9. Woltring H.J., et al.: Instantaneous helical axis estimation via natural, cross-validated splines. In: *Biomechanics: basics and applied research (Developments in biomechanics)* Vol. 3, pp. 121–128, Springer, Berlin (1987).
10. Ferraresi C., et al.: In-vivo analysis of ankle joint movement for patient-specific kinematic characterization. *Proc Inst Mech Eng H* 231(9), 831–838 (2017).
11. Leardini A., et al.: A new anatomically based protocol for gait analysis in children. *Gait & Posture* 26(4), 560–571 (2007).
12. Ferraresi C., et al., inventors; Politecnico di Torino (IT), Istituto Ortopedico Rizzoli (IT), assignee. Articulated Ankle-Foot Orthosis with a floating axis of rotation. PCT patent No. WO/2017/199108 (A1), (2017).
13. Telfer S., et al.: Embracing additive manufacture: implications for foot and ankle orthosis design. *BMC Musculoskeletal Disorders* 13:84 (2012).
14. Chen R. K., et al.: Additive manufacturing of custom orthoses and prostheses—A review. *Additive Manufacturing* 12 (Part A), 77–89 (2016).